UC Riverside

UC Riverside Previously Published Works

Title

Targeted Proteomic Profiling Revealed Roles of Small GTPases during Osteogenic Differentiation.

Permalink

Journal

Authors

Yang, Yen-Yu
Soh, Ruthia
Vera-Colón, Madeline
et al.

Publication Date

DOI

Targeted Proteomic Profiling Revealed Roles of Small GTPases during Osteogenic Differentiation

Yen-Yu Yang,

Department of Chemistry, University of California, Riverside, Riverside, California 92521-0403, United States

Ruthia Soh,

Department of Molecular, Cell, and Systems Biology, University of California, Riverside, Riverside, California 92521-0403, United States

Madeline Vera-Colón,

Environmental Toxicology Graduate Program, University of California, Riverside, Riverside, California 92521-0403, United States

Ming Huang,

Environmental Toxicology Graduate Program, University of California, Riverside, Riverside, California 92521-0403, United States

Nicole I. zur Nieden,

Department of Molecular, Cell, and Systems Biology and Environmental Toxicology Graduate Program, University of California, Riverside, Riverside, California 92521-0403, United States

Yinsheng Wang

Department of Chemistry, University of California, Riverside, Riverside, California 92521-0403, United States; Environmental Toxicology Graduate Program, University of California, Riverside, Riverside, California 92521-0403, United States

Abstract

The small GTPase superfamily of proteins are crucial for numerous cellular processes, including early development. The roles of these proteins in osteogenic differentiation, however, remained poorly explored. In this study, we employed a high-throughput targeted proteomic method, relying on scheduled liquid chromatography–multiple-reaction monitoring (LC-MRM) coupled with synthetic stable isotope-labeled peptides, to interrogate systematically the temporal responses of the entire small GTPase proteome during the course of osteogenic differentiation of H9 human embryonic stem cells. Our results demonstrated that the method offers high quantification

accuracy, reproducibility, and throughput. In addition, the quantification results revealed altered expression of a large number of small GTPases accompanied with osteogenic differentiation, especially those involved with autophagy. We also documented a previously unrecognized role of KRAS in osteogenesis, where it regulates the accumulation of extracellular matrix for mineralization through attenuating the activity of secreted matrix metalloproteinase 9 (MMP9). Together, this study represents a novel application of a state-of-the-art analytical method, i.e., targeted quantitative proteomics, for revealing the progressive reprogramming of the small GTPase proteome during osteogenic differentiation of human embryonic stem cells, and our results revealed KRAS as a new regulator for osteogenesis.

Graphical Abstract
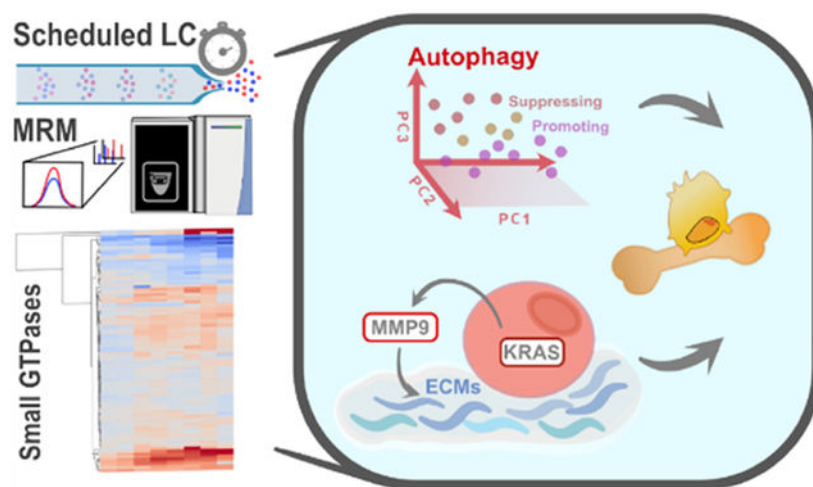
INTRODUCTION

Bone remodeling is a continuous and active process throughout adulthood that maintains the integrity of the skeletal system.[1,2] Optimal osteogenic differentiation is essential for health; excessive and inadequate osteogenesis, however, can result in heterotopic ossification and osteoporosis, respectively.[2,3] At the cellular level, osteoblasts are derived from mesenchymal stem cells (MSCs) in adults,[4,5] where osteogenesis of MSCs could be activated by circulating hormones and locally generated cytokines and/or growth factors, e.g., the secreted transforming growth factor β (TGF-β).[6–8] Notably, depending on extracellular stimuli and downstream signaling events, the MSCs can also be differentiated into other lineages, e.g., adipocytes, chondroblasts, and myoblasts.[9] Thus, understanding the molecular mechanisms of osteoblast differentiation and maturation is crucial for understanding the pathogenesis of bone diseases.

Small GTPases of the Ras superfamily are molecular switches that undergo conformational changes between the guanosine triphosphate (GTP)-associated active state and the guanosine diphosphate (GDP)-bound inactive state.[10–12] When bound with GTP, these proteins interact with downstream effector proteins to modulate diverse cellular processes, including cell differentiation, growth, and proliferation.[13,14] Previous studies revealed the involvement

of small GTPases in regulating osteogenesis. CDC42, for instance, was found to promote osteogenesis in adult bone-marrow-derived MSCs.[15] In addition, the intraflagellar transport protein 80 (IFT80) is upregulated during osteogenic differentiation *in vivo*, where genetic depletion of IFT80 diminished the expression of osteoblast regulatory genes (e.g., *Runx2*) upon osteogenesis of murine MSCs.[16]

Despite the earlier evidence supporting the roles of small GTPases in modulating osteogenesis, the global picture of their functions in osteogenic differentiation remains poorly investigated. We reason that a systematic analysis of the expression of the entire small GTPase proteome during osteogenesis could offer mechanistic insights into osteogenic differentiation. Unlike the conventional data-dependent acquisition (DDA)-based discovery proteomic analysis, targeted proteomic analysis on triple-quadrupole mass spectrometers operated in the multiple-reaction monitoring (MRM) mode provides excellent sensitivity, reproducibility, and accuracy in protein quantification.[17,18] Targeted proteomics was found to afford increased depth in proteome coverage compared to the DDA mode.[19]

Here, we documented the first application of a state-of-the-art analytical method, i.e., an MRM-based targeted proteomic approach together with the use of synthetic stable isotope-labeled peptides as internal standards, to explore systematically the roles of small GTPases in osteogenic differentiation. We were able to quantify more than 50% of the small GTPase proteome in H9 human embryonic stem cells (hESCs) and C3H10T1/2 murine mesenchymal progenitor cells (mMPCs),[19,20] demonstrating the high sensitivity of the analytical method. Importantly, the present study also highlighted the throughput of the method, where the entire small GTPase proteome could be monitored by LC-MS/MS in a single run. Our results suggest that stem cells coordinate the expression of small GTPases to modulate autophagy, thereby promoting osteogenic differentiation. We also found that KRAS regulates osteogenesis through attenuating matrix metalloproteinase 9 (MMP9)-mediated degradation of extracellular matrix (ECM).

EXPERIMENTAL SECTION

Cell Culture and Transfection.

C3H10T1/2 cells were cultured in Dulbecco's modified Eagle's medium (DMEM, Thermo Fisher) supplemented with 10% fetal bovine serum (FBS, Thermo Fisher) and 1% penicillin–streptomycin solution (100 IU/mL, GE Healthcare). The cells were maintained at 37 °C in a humidified chamber supplemented with 5% CO_2. Osteogenesis was induced as described elsewhere.[21] Briefly, confluent C3H10T1/2 cells were refreshed with osteogenesis medium (complete DMEM supplemented with 50 μg/mL sodium ascorbate, 10 mM β-glycerophosphate, and 200 ng/mL recombinant BMP2 protein) every 72 h for 7 days. All experiments were conducted for cells within 15 passages.

H9 hESCs (WiCell) were cultured on a Matrigel (BD Bioscience)-coated surface in mTeSR plus medium (Stem Cell Technologies). The cells were maintained at 37 °C in a humidified chamber supplemented with 5% CO_2. To subculture, cell colonies were treated with accutase (Innovative Cell Technologies) for 30 s followed by scraping. The colonies were seeded into fresh culture medium at a 1:6 ratio (v/v). Differentiation was initiated as described

previously.[22] Briefly, cells at confluence were incubated in DMEM supplemented with 15% FBS (Atlanta Biologicals), 0.5% penicillin–streptomycin (Gibco), 1% non-essential amino acids (Gibco), and 0.1 mM β-mercaptoethanol (Sigma) for 5 days. Osteogenesis was further induced by supplementing the culture medium with 50 μg/mL sodium ascorbate (Sigma), 10 mM β-glycerophosphate, and 0.12 μM vitamin D_3 for 15 days. Confluent cells prior to differentiation induction were collected at day 0 as the undifferentiated control and the cells with differentiation/osteogenesis induction were collected at the indicated time points.

Cell Lysis and Proteomic Sample Preparation.

Cells were lysed in ice-chilled CelLytic M cell lysis reagent (Sigma) containing 1% protease inhibitor cocktail (Sigma). The cell lysate was subsequently centrifuged at 16 000g for 30 min at 4 °C to remove debris. Supernatants containing total proteins were quantified using Quick Start Bradford Protein Assay (Bio-Rad). Total proteins were mixed with 4× Laemmli SDS loading buffer (Bio-Rad), and the resulting mixtures were boiled for 5 min. Approximately 50 μg of total proteins were resolved on a 14% SDS-PAGE gel and subsequently stained with Coomassie Brilliant Blue R-250.

Proteins were digested in-gel as described previously.[23,24] Briefly, gel bands corresponding to the molecular weight range of 15–37 kDa were excised and cut into 1 mm^3 cubes. The gel pieces were destained sequentially with 25 and 50% acetonitrile in 50 mM ammonium bicarbonate (pH 7.8). Cysteines in proteins were reduced and alkylated by incubating the gel pieces in 10 mM dithiothreitol (DTT) at 37 °C for 1 h and 55 mM iodoacetamide at room temperature in the dark for 20 min, respectively. The proteins were digested in-gel with trypsin in 50 mM ammonium bicarbonate (pH 7.8) at 37 °C for 18 h at an enzyme/protein ratio of 1:100. Peptides were extracted from the gel pieces by shaking sequentially in 5 and 50% acetonitrile containing 5% acetic acid. The resulting tryptic peptides were desalted with C18 ZipTip (Agilent) and reconstituted in 0.1% formic acid.

Approximately 8% of the digestion mixture was spiked-in with a crude pool of synthetic stable isotope-labeled (SIL) small GTPase peptides (4 fmol each) with a C-terminal [$^{13}C_6$,$^{15}N_2$]-labeled lysine (+8.0 Da) or [$^{13}C_6$,$^{15}N_4$]-labeled arginine (+10 Da). The SIL peptides were synthesized by New England Peptides (Cambridge, MA) at 1.0 μmol scale in a 96-well plate format, where the average purity of the peptides was estimated to be 75% according to the vendor. The synthetic SIL peptides were reconstituted with 0.1% formic acid, mixed to give a stock solution, which was spiked into each sample at a concentration of ~ 2 fmol/μL for each peptide.

Liquid Chromatography–Tandem Mass Spectrometry (LC-MS/MS).

The MRM-based LC-MS/MS experiments were performed on a TSQ Altis triple-quadrupole mass spectrometer (Thermo) coupled with an UltiMate 3000 UPLC (Thermo) and a Flex nanoelectrospray ion source (Thermo). The spiked-in sample was loaded onto a trapping column (3 cm, 150 μm ID) packed in-house with C18 resin (5 μm in particle size and 120 Å in pore size, Dr. Maisch GmbH HPLC) at a flow rate of 3 μL/min. The peptides were eluted from the trapping column and resolved on an ~ 25 cm analytical column (75 μm i.d.) packed with C18 resin (3 μm in particle size and 120 Å in pore size, Dr. Maisch GmbH

HPLC) using a gradient of 12–40% buffer B (0.1% formic acid and 80% acetonitrile). The flow rate of elution was 0.3 μL/min. The spray voltage was 2 kV, and the ion transfer tube temperature was set at 320 °C. The resolution for Q1 and Q3 was set at 0.7 m/z in full width at half-maximum (FWHM). Collision-induced dissociation (CID) in Q2 was conducted in 1.5 mTorr argon, where the relative collision energy was set as default in Skyline (version 19.1.0.193).[25–27]

The mass spectrometer was scheduled to monitor precursor–product ion transitions for each of the 147 and 137 human and mouse unique small GTPase peptides, respectively, where each small GTPase was represented by a unique tryptic peptide. The three most abundant y ions detected in MS/MS obtained from data-dependent acquisition (DDA) mode were selected for the quantification of each peptide (i.e., 3 MRM transitions were selected for each small GTPase peptide).[19] Cycle time was 3 s, and the retention time (RT) window for each peptide was 3.5 min. The retention times of the eluted peptides were predicted from their normalized retention times (iRT), and the iRT-RT linear regression was determined from 9 tryptic peptides of BSA.[28,29]

The DDA analysis was conducted on a Fusion Lumos Orbitrap tribrid mass spectrometer (Thermo) coupled with an Easy 1000 nLC (Thermo) and a Flex nanoelectrospray ion source (Thermo). The mass spectrometer was equipped with a high-field asymmetric-waveform ion mobility spectrometry (FAIMS), where the compensation voltages (CV) were set at −40, −60, and −80 V. The carrier gas flow was set at 4.2 L/min. The cycle time was 3 s with each CV being scanned for 1 s. The LC conditions were the same as those described for LC-MRM analysis except that a 160-min linear gradient of 12–34% buffer B was employed. The spray voltage was set as 2 kV, and the ion transfer tube temperature was 320 °C. MS was acquired with Orbitrap at a resolution of 60 000. Fragmentation was conducted with higher-energy collisional dissociation (HCD) at a relative collisional energy of 30. The MS/MS were acquired in the linear ion trap, where the scan rate was set as rapid.

MRM Data Analysis.

All extracted-ion chromatograms (XICs) were manually inspected and filtered with dot-product (dotp) being >0.7. The peak areas of all of the three monitored product ions were summed for each small GTPase peptide, and the total peak area was subsequently normalized against that for the corresponding spiked-in heavy isotope-labeled peptide to represent the relative ratio of the peptide and the corresponding small GTPase for each LC-MRM analysis. The resulting ratio of the differentiated cells was further normalized against that of the undifferentiated cells for the relative quantifications of small GTPases upon osteogenic differentiation.

For H9 hESCs, the protein lysates from each biological replicate were processed (i.e., with SDS-PAGE fractionation, ingel digestion, and stable isotope-labeled peptide addition) on two separate days, and the ratios obtained from the two technical replicates were averaged to represent the ratio for the biological replicate. In addition, samples from each technical replicate were analyzed by LC-MRM twice, and the ratios obtained from the two LC-MRM runs were averaged to yield the protein ratio for the technical replicate. A total of three and two biological replicates were conducted for the C3H10T1/2 and H9 cells, respectively.

The mass spectrometry proteomics data are deposited to the ProteomeXchange Consortium via the PRIDE[30] partner repository with the dataset identifier (PXD038467) and Panorama (https://panoramaweb.org/pTMsXN.url).

RESULTS

Scheduled LC-MRM Analysis Revealed Altered Expression of Small GTPases during Osteogenic Differentiation of H9 hESCs.

Previous studies revealed the roles of several small GTPases, e.g., CDC42 and IFT80, in osteogenesis.[13,31] Nevertheless, the global picture of the involvement of small GTPases in osteogenic differentiation remains largely unexplored. Here, we aim to investigate comprehensively the differential expression of small GTPases during the entire time course of osteogenic differentiation. To achieve high coverage of the small GTPase proteome and to improve quantification accuracy, we implemented a scheduled MRM-based targeted proteomic approach coupled with the use of synthetic stable isotope-labeled standard peptides (Figure 1A).[20] The same elution time and fragmentation patterns of the endogenous small GTPase peptide as its stable isotope-labeled counterpart enable robust identification and quantification of small GTPase proteins. To minimize cost and to improve analytical throughput, we selected one unique peptide to represent each small GTPase. In this vein, the primary sequences for some small GTPases are quite similar; thus, care was taken to ensure that the peptide chosen for quantifying each small GTPase is uniquely present in the protein; another criterion for peptide selection is that it could be reproducibly detected in multiple cell lines by LC-MS/MS analysis.[19,20]

ESCs can be differentiated progressively into osteoblasts (Figure S1A).[32,33] To examine the dynamic expression of small GTPases during osteogenic differentiation, we collected cells on different days throughout the differentiation time course (i.e., on days 3, 5, 6, 8, 12, 15, and 20 following osteogenesis induction) for LC-MRM analysis (Figure S1B–C). Together, we identified 93 small GTPases, which represent ~ 60% of the human small GTPase proteome (Figure 1B), in a single 60 min LC-MS/MS run, highlighting the throughput of the method. The majority of the identified small GTPases were detected in both biological replicates, with 83 proteins being commonly quantified (Figure 1C). Moreover, the quantification results are highly consistent between the two biological replicates (Figures 2A and S2), suggesting the excellent reproducibility of the method.

To better characterize the dynamic expression of small GTPases and reveal their roles in regulating osteogenic differentiation, we conducted a hierarchical clustering analysis based on their relative expression with respect to undifferentiated cells (i.e., day 0). The expression profiles for day 3 and day 5 are similar, but are distinct from cells collected after day 6 (Figures 2B and S3). Interestingly, this distinction is consistent with the critical time points in osteogenic differentiation (Figure S1A). In this vein, H9 cells were withdrawn from pluripotency upon differentiation induction at day 0 and the osteogenesis was further induced starting at day 5. Our results showed that the expression of a large subset of small GTPases was modulated during the initial differentiation and further systemically altered upon osteogenic induction. To confirm the proteomic results, we conducted Western blot analysis for selected small GTPases (Figure 2C,D). The quantification results obtained from

the two orthogonal methods are highly consistent with $R^2 > 0.8$ (Figure 2E), underscoring the quantification accuracy of the LC-MRM method.

Among the quantified small GTPases, RAB32 was continuously upregulated during the entire time course of osteogenic differentiation (Figure 2A,B). On the other hand, we observed previously diminished expression of RAB32 upon adipogenic differentiation of mMPCs, including 3T3-L1 and C3H10T1/2 cells,[13] suggesting an important role of this small GTPase in modulating cell fate decision. The expression of KRAS, on the other hand, was increased during germ layer differentiation, but diminished at later time points during osteogenic differentiation from MPCs (Figures 2A and S4), suggesting that the protein may assume multiple roles in different phases of the differentiation process. Other small GTPases, e.g., RAB27B and RAB33A, are up- and downregulated, respectively (Figure 2A,B), throughout the course of differentiation from ESCs to osteoblasts. The results suggest that different small GTPases may assume distinct roles in the osteogenic differentiation of stem cells.

Validation of Small GTPase Expression in Murine C3H10T1/2 mMPCs.

Our aforementioned proteomic results demonstrated the potential roles of small GTPases in the osteogenic differentiation of H9 human hESCs. To identify small GTPases with general roles in osteogenesis, we further conducted LC-MRM analysis to explore the osteogenesis-induced differential expression of small GTPases in C3H10T1/2 mMPCs.[21] We confirmed the successful differentiation of C3H10T1/2 cells to osteoblasts by Alizarin Red S staining and by quantifying Alizarin Red S dye extracted from the stained cells (Figure S5A). The successful osteogenesis of C3H10T1/2 cells was also manifested by the mRNA expression levels of osteogenesis markers, including *Runx2* and *Ocn* (Figure S5B).

We next monitored the relative expression levels of small GTPases in differentiated and undifferentiated C3H10T1/2 cells using LC-MRM, and our results led to the quantification of 74 small GTPases, representing >50% of the murine small GTPase proteome (Figure 3A), again highlighting the sensitivity of the analytical platform in quantifying small GTPase proteome. Among the quantified small GTPases, 23 were differentially expressed by at least 1.5-fold based on at least two biological replicates (Figure 3B,C), suggesting their potential involvement in regulating osteogenic differentiation from mMPCs. We next conducted Western blot analysis for selected small GTPases (Figure S6A,B), and the quantification results are again highly consistent with those obtained from LC-MRM analysis (Figure S6C), validating the quantification accuracy of the LC-MRM method. Among the commonly identified proteins in H9 hESCs and C3H10T1/2 mMPCs, KRAS was consistently downregulated upon osteogenic differentiation from the mesenchymal stage (i.e., day 6 to day 20 for H9 cells) in both cell lines (Figures 2A and 3C). On the other hand, RAB32 was commonly upregulated, suggesting its potential roles as a master regulator for mMPC differentiation.[13]

Autophagy-Regulating Small GTPases Are Differentially Expressed during Osteogenesis of H9 hESCs.

Autophagy, which recycles nonessential or damaged macromolecules and organelles, is a conserved degradation pathway in cells upon encountering stress.[34] Previous studies showed that autophagy is necessary for osteoblast differentiation.[35,36] Interestingly, many small GTPases are known to regulate autophagy. For instance, RAB27B and RAB33A were documented to promote and inhibit autophagy, respectively.[37–39] In line with this notion, our MRM results revealed up- and downregulations of RAB27B and RAB33A during osteogenesis, respectively (Figure 2A,B), which were further confirmed by Western blot analysis (Figure 2C,D).

Next, we performed principal component analysis (PCA) for the small GTPases quantified by LC-MRM based on their relative expression to day 0 throughout the differentiation time course. The small GTPases were further categorized according to their known functions in autophagy. Strikingly, small GTPases that promote, inhibit, or exhibit no reported functions in autophagy are distinctly separated in the PCA plot (Figure S7), suggesting that hESCs may orchestrate the expression of small GTPases to modulate autophagy for successful osteogenic differentiation.

KRAS Regulates Osteogenesis through Modulating the Integrity of Extracellular Matrix.

We observed diminished KRAS expression upon mesenchymal differentiation to osteoblasts in both H9 hESCs and C3H10T1/2 mMPCs (Figures 2A and 3C). Thus, we hypothesized that reduced expression of KRAS might promote osteogenesis. To test this hypothesis, we overexpressed KRAS in H9 hESCs by using a lentiviral system. Interestingly, the calcification rate was significantly diminished in cells transfected with lentivirus on day 4, which led to overexpression of KRAS starting on ~day 7 (Figure 4A,B). Consistently, we observed a decreased expression of osteocalcin, a protein secreted by mature osteoblasts to assist calcification of extracellular matrix, in these cells (Figure 4C). Cells transfected at day 10, which led to overexpression of KRAS starting on day 13, however, did not confer any apparent effect on osteogenesis rate. During the osteogenesis of H9 hESCs, day 7 and day 13 correspond to the stage of MSCs and the time of differentiation of osteoprogenitor cells into osteoblasts, respectively (Figure S1A). One possible explanation for the differential effects elicited by KRAS overexpression on different days following osteogenesis induction is that KRAS is crucial for MSCs, but assumes a less significant role after they become osteoprogenitor cells. To confirm that decreased KRAS expression is required for osteogenesis from MSCs, we overexpressed KRAS in C3H10T1/2 cells (Figure 4D). Similar to the findings made for H9 hESCs, we observed decreased calcification and diminished expression of *Ocn* transcripts in KRAS-overexpressing cells (Figures 4E,F and S8). Together, our results demonstrated that attenuated KRAS expression is required for optimal osteogenic differentiation from a mesenchymal state.

KRAS was previously shown to regulate the integrity of the extracellular matrix through modulating the activities of matrix metalloproteinases (MMPs).[40,41] Notably, extracellular matrix is involved in the differentiation and maturation of bone tissues. Collagens, especially type-I collagen, are secreted by osteoblasts and further mineralized by calcium phosphate

deposition, and subsequently crystallize with hydroxyapatite.[42,43] Given that KRAS could stimulate the activities of MMPs, diminished expression of KRAS during osteogenesis from mesenchymal cells may be a crucial step toward the formation of mineralized matrices. To examine this possibility, we collected conditioned media for gelatin zymography analysis, and our results showed that MMP9, whose identity was confirmed by LC-MS/MS analysis, displayed elevated activities upon osteogenic differentiation (Figure S9A,B). Next, we analyzed secreted MMP activity from KRAS-overexpressing H9 hESCs or C3H10T1/2 mMPCs. Interestingly, we observed augmented MMP9 activity in cells overexpressing KRAS (Figures 4G and S9C). In this vein, previous studies revealed that MMP9 could digest type-I collagen, which is the predominant protein in the extracellular matrix for osteoblast mineralization.[44] Together, our LC-MRM results revealed decreased KRAS expression upon mesenchymal differentiation toward osteoblast, and we observed that diminished KRAS is crucial for ECM accumulation.

DISCUSSION

Small GTPases are among the most important regulators in signal transduction in cells. Earlier studies documented the important roles of a few small GTPases in osteogenesis.[15,16] The expression of the entire superfamily of small GTPase proteins during osteogenic differentiation, however, remained largely unexplored owing to the lack of appropriate techniques.

Here, we employed a recently developed scheduled LC-MRM-based targeted proteomic method, coupled with synthetic stable isotope-labeled peptides,[20] to interrogate the dynamic changes in expression of the entire small GTPase proteome during osteogenesis. We were able to identify ~90 small GTPases and quantify over 50% of the small GTPase proteome, suggesting the excellent sensitivity of the method (Figures 1B and 2A). In addition, scheduled LC-MRM offered high throughput, where we were able to monitor ~90% of the small GTPase proteome in a single 60-min LC-MS/MS run. We also revealed that the method provided high accuracy, as validated by western blot analysis (Figures 2C and S6C).

It is worth noting that H9 cells are ESCs, which, upon withdrawal from pluripotency, are differentiated sequentially into germ layers, MPCs, osteoprogenitor cells, and finally into osteoblasts (Figure S1A). Therefore, our systematic profiling revealed dynamic expression of the small GTPase proteome upon osteogenic differentiation from as early as the embryonic stages, and the proteomic results obtained from this study may enable future investigations about the functions of small GTPases in different stages of differentiation.

Our results validated some known small GTPases in regulating osteogenic differentiation. CDC42, for instance, was shown to promote osteogenesis of MSCs isolated from adult bone marrow.[15] Here, we observed increased CDC42 expression in H9 cells at day 6 post-induction, at which point mesenchymal cells are differentiated into osteoprogenitor cells (Table S3). In addition, our proteomic results showed that the expression of RAB32 was upregulated during osteogenic differentiation of both H9 hESCs (Figure 2B,C) and C3H10T1/2 mMPCs (Figure 3B,C). Interestingly, we found previously that diminished RAB32 expression is required for successful adipogenesis, which is an alternative

differentiation lineage for mesenchymal cells.[13] The fact that RAB32 protein expression displays opposite trends in osteogenesis and adipogenesis suggests that RAB32 could be a very important regulator of mesenchymal cell differentiation.

Emerging lines of evidence suggest that an appropriate level of autophagy promotes the differentiation and survival of osteoblasts derived from various stem cells.[35,36] An earlier genome-wide analysis of patients with defects in bone density of wrist underscored an association of autophagy with osteoporosis.[45] While previous studies documented the roles of small GTPases in the initiation and maturation of autophagy, little is known about their involvement in mediating autophagy during osteogenic differentiation. Here, our PCA results revealed that the autophagy-promoting, -suppressing, and -unrelated small GTPases are clustered together (Figure S7). In addition, we observed the up- and downregulations of RAB27B and RAB33A, respectively, during osteogenesis (Figure 2A,C), which is in keeping with previous findings that RAB27B and RAB33A could promote and suppress autophagy, respectively.[37,46] Thus, stem cells may coordinate the expression of these small GTPases to modulate autophagy during osteogenesis.

We also revealed an attenuated expression of KRAS during osteogenic differentiation of mesenchymal cells (Figures 2A and 3B), and diminished KRAS expression is commonly required for mesenchymal differentiation of H9 hESCs and C3H10T1/2 mMPCs to osteoblasts (Figure 4A,B,E). KRAS was previously shown to regulate ECM integrity through modulating MMP activity, where elevated expression and/or activation of KRAS lead to collagen degradation, thereby promoting the migration and invasion of cancer cells.[40,41] In addition, extracellular matrix, e.g., type-I collagen, is actively secreted during osteogenesis, and deposited type-I collagen further mineralizes to allow ossification.[43] Our results showed that KRAS was downregulated during the differentiation of mesenchymal cells to osteoblasts. Hence, stem cells may modulate the expression of KRAS for extracellular matrix accumulation.

Our zymography assay results revealed diminished MMP9 activity during osteogenesis (Figure S9A) and augmented MMP9 activity in cells overexpressing KRAS (Figures 4G and S9C). On the grounds that MMP9 was found to degrade type-I collagen,[44] attenuated MMP9 activity arising from diminished KRAS expression may be crucial for osteogenesis. Interestingly, we observed decreased calcification in H9 cells overexpressing KRAS when transduced at day 4, but not at day 10 (Figure 4A). Cells transfected at day 4 following differentiation induction would start to overexpress KRAS when cells were undergoing osteogenic differentiation from mesenchymal stage (i.e., day 6). Previous studies showed that ECMs deposited during osteogenesis could initiate a positive feedback loop to promote MSC differentiation,[47,48] and osteogenesis imperfecta is associated with mutations in genes with functions in maintaining ECM integrity.[42] Our study, hence, revealed a novel KRAS-MMP9-mediated pathway, which promotes osteogenesis via remodeling ECMs.

To our knowledge, this represents the first application of an MRM-based targeted proteomic method for revealing the roles of small GTPases in osteogenic differentiation. Our results reinforced the notion that scheduled LC-MRM analysis, together with synthetic stable isotope-labeled peptides, offered excellent sensitivity, reproducibility, and throughput

in quantifying the expression levels of small GTPase proteins.[20] We characterized systematically the involvements of small GTPases in osteogenesis, and our results validated the earlier findings and unveiled previously uncharacterized roles of small GTPases in osteogenesis. We showed that osteogenic differentiation is accompanied with substantial alterations in expression of a number of small GTPases with functions in autophagy. We also discovered a crucial role of KRAS in regulating ECM accumulation for optimal osteogenesis. Downregulating KRAS expression, which attenuates MMP9 activity so as to promote ECM accumulation and mineralization, is commonly observed in the two distinct cell lines studied herein. Our findings provide important knowledge basis for future therapeutic interventions of human diseases emanating from aberrant osteogenic differentiation, e.g., osteogenesis imperfecta.

It is worth discussing the limitations of the present study. First, methionine-containing peptides were selected for the quantification of several small GTPases (i.e., RHOA, RAC3, RAB26, RAB2A, RAB26, RAB37, RAB6A, RAD, and REM2) to fulfill the selection criteria, including being unique to the small GTPases and reproducibly detected in multiple cell lines. However, differential oxidation of methionine among samples may affect the quantification results of these small GTPases, and alternative methods (e.g., Western blot analysis) should be employed to validate the quantification results of these proteins. Second, post-translational modifications (PTMs) may shift some small GTPases outside from the excised gel region (i.e., 15–37 kDa), thereby preventing their detection. To minimize cost and to enhance analytical throughput, we employed a single unique peptide for quantifying each small GTPase protein. Differential PTMs occurring on amino acids in these peptides at different time points of osteogenic differentiation may also affect the quantification accuracy of these small GTPases. Third, we aimed to monitor the changes in small GTPase proteome at nine different time points along the course of osteogenic differentiation of H9 ESCs; thus, we only conducted the osteogenic differentiation in two biological replicates. While incorporating more biological replicates would have improved further the robustness of study, our analytical workflow of incorporating multiple technical replicates for each biological replicate (i.e., the samples from each biological replicate were analyzed by SDS-PAGE and in-gel tryptic digestion twice on two separate days, and each digestion mixture was analyzed by LC-MRM twice) enhances the robustness of the quantification results. This is indeed supported by the fact that the data acquired from the two biological replicates are highly consistent (Figures 2 and S2).

Supplementary Material

Refer to Web version on PubMed Central for supplementary material.

ACKNOWLEDGMENTS

REFERENCES

(1). Infante A; Rodriguez CI Stem Cell Res. Ther 2018, 9, 244. [PubMed: 30257716]

(2). Raggatt LJ; Partridge NC J. Biol. Chem 2010, 285, 25103–25108. [PubMed: 20501658]

(3). Meyers C; Lisiecki J; Miller S; Levin A; Fayad L; Ding C; Sono T; McCarthy E; Levi B; James AW JBMR Plus 2019, 3, No. e10172.

(4). Grottkau BE; Lin Y Bone Res. 2013, 1, 133–145. [PubMed: 26273498]

(5). Zhang L; Jiao G; Ren S; Zhang X; Li C; Wu W; Wang H; Liu H; Zhou H; Chen Y Stem Cell Res. Ther 2020, 11, 38. [PubMed: 31992369]

(6). Wu M; Chen G; Li YP Bone Res. 2016, 4, 16009. [PubMed: 27563484]

(7). Xu C; Wang J; Xie X; Zhao H; Carpenter E; Feng J FASEB J. 2021, 35, No. e05019.

(8). Infante A; Cabodevilla L; Gener B; Rodriguez CI Front. Cell Dev. Biol 2022, 10, No. 830928.

(9). Andrzejewska A; Lukomska B; Janowski M Stem Cells 2019, 37, 855–864. [PubMed: 30977255]

(10). Vetter IR; Wittinghofer A Science 2001, 294, 1299–1304. [PubMed: 11701921]

(11). Wennerberg K; Rossman KL; Der CJ J. Cell Sci 2005, 118, 843–846. [PubMed: 15731001]

(12). Mishra AK; Lambright DG Biopolymers 2016, 105, 431–448. [PubMed: 26972107]

(13). Yang YY; Huang M; Wang Y Anal. Chem 2020, 92, 6756–6763. [PubMed: 32237738]

(14). Villarroel-Campos D; Bronfman FC; Gonzalez-Billault C Cytoskeleton 2016, 73, 498–507. [PubMed: 27124121]

(15). Gao L; Gorski JL; Chen CS Am. J. Pathol 2011, 178, 969–974. [PubMed: 21356349]

(16). Yang S; Wang C Bone 2012, 51, 407–417. [PubMed: 22771375]

(17). Shi T; Song E; Nie S; Rodland KD; Liu T; Qian WJ; Smith RD Proteomics 2016, 16, 2160–2182. [PubMed: 27302376]

(18). Ebhardt HA; Root A; Sander C; Aebersold R Proteomics 2015, 15, 3193–3208. [PubMed: 26097198]

(19). Huang M; Qi TF; Li L; Zhang G; Wang Y Cancer Res. 2018, 78, 5431–5445. [PubMed: 30072397]

(20). Huang M; Darvas M; Keene CD; Wang Y Anal. Chem 2019, 91, 12307–12314. [PubMed: 31460748]

(21). Mukherjee A; Rotwein PJ Cell Sci. 2009, 122, 716–726.

(22). Martinez IK; Bhanu B; zur Nieden NI MethodsX 2021, 8, No. 101265.

(23). Shevchenko A; Tomas H; Havlis J; Olsen JV; Mann M Nat. Protoc 2006, 1, 2856–2860. [PubMed: 17406544]

(24). Gao Z; Yang YY; Huang M; Qi TF; Wang H; Wang Y Anal. Chem 2022, 94, 14925–14930. [PubMed: 36264766]

(25). MacLean B; Tomazela D; Shulman N; et al. Bioinformatics 2010, 26, 966–968. [PubMed: 20147306]

(26). Pino LK; Searle BC; Bollinger JG; Nunn B; MacLean B; MacCoss MJ Mass Spectrom. Rev 2020, 39, 229–244. [PubMed: 28691345]

(27). Maclean B; Tomazela DM; Abbatiello SE; Zhang S; Whiteaker JR; Paulovich AG; Carr SA; Maccoss MJ Anal. Chem 2010, 82, 10116–10124. [PubMed: 21090646]

(28). Xiao Y; Guo L; Wang Y Mol. Cell. Proteomics 2014, 13, 1065–1075. [PubMed: 24520089]

(29). Escher C; Reiter L; MacLean B; Ossola R; Herzog F; Chilton J; MacCoss MJ; Rinner O Proteomics 2012, 12, 1111–1121. [PubMed: 22577012]

(30). Perez-Riverol Y; Bai J; Bandla C; Garcia-Seisdedos D; Hewapathirana S; Kamatchinathan S; Kundu DJ; Prakash A; Frericks-Zipper A; Eisenacher M; Walzer M; Wang S; Brazma A; Vizcaino JA Nucleic Acids Res. 2022, 50, D543–D552. [PubMed: 34723319]

(31). Pavlos NJ; Cheng TS; Qin A; Ng PY; Feng HT; Ang ES; Carrello A; Sung CH; Jahn R; Zheng MH; Xu J Mol. Cell. Biol 2011, 31, 1551–1564. [PubMed: 21262767]

(32). Sparks NRL; Martinez IKC; Soto CH; zur Nieden NI Stem Cells 2018, 36, 349–362. [PubMed: 29193426]

(33). zur Nieden NI; Kempka G; Ahr HJ Differentiation 2003, 71, 18–27. [PubMed: 12558600]

(34). Yim W-Y; Mizushima N Cell Discovery 2020, 6, 6. [PubMed: 32047650]

(35). Wan Y; Zhuo N; Li Y; Zhao W; Jiang D Biochem. Biophys. Res. Commun 2017, 488, 46–52. [PubMed: 28476617]

(36). Yin X; Zhou C; Li J; Liu R; Shi B; Yuan Q; Zou S Bone Res. 2019, 7, 28. [PubMed: 31666998]

(37). Underwood R; Wang B; Carico C; Whitaker RH; Placzek WJ; Yacoubian TA J. Biol. Chem 2020, 295, 8005–8016. [PubMed: 32350025]

(38). Sekar M; Thirumurugan K Mol. Cell. Biochem 2022, 477, 727–742. [PubMed: 35022960]

(39). Lu Q; Wang PS; Yang L Cell Biosci. 2021, 11, 35. [PubMed: 33557950]

(40). Wang G; Yin L; Peng Y; Gao Y; Gao H; Zhang J; Lv N; Miao Y; Lu Z Cell Proliferation 2019, 52, No. e12575.

(41). Justilien V; Regala RP; Tseng IC; Walsh MP; Batra J; Radisky ES; Murray NR; Fields AP PLoS One 2012, 7, No. e35040.

(42). Lin X; Patil S; Gao YG; Qian A Front. Pharmacol 2020, 11, 757. [PubMed: 32528290]

(43). Schlesinger PH; Blair HC; Beer Stolz D; Riazanski V; Ray EC; Tourkova IL; Nelson DJ Am. J. Physiol. – Cell Physiol 2020, 318, C111–C124. [PubMed: 31532718]

(44). Bigg HF; Rowan AD; Barker MD; Cawston TE FEBS J. 2007, 274, 1246–1255. [PubMed: 17298441]

(45). Zhang L; Guo YF; Liu YZ; Liu YJ; Xiong DH; Liu XG; Wang L; Yang TL; Lei SF; Guo Y; Yan H; Pei YF; Zhang F; Papasian CJ; Recker RR; Deng HW J. Bone Miner. Res 2010, 25, 1572–1580. [PubMed: 20200951]

(46). Itoh T; Fujita N; Kanno E; Yamamoto A; Yoshimori T; Fukuda M Mol. Biol. Cell 2008, 19, 2916–2925. [PubMed: 18448665]

(47). Harvestine JN; Vollmer NL; Ho SS; Zikry CA; Lee MA; Leach JK Biomacromolecules 2016, 17, 3524–3531. [PubMed: 27744699]

(48). Zhang Z; Luo X; Xu H; Wang L; Jin X; Chen R; Ren X; Lu Y; Fu M; Huang Y; He J; Fan Z Cell Biol. Int 2015, 39, 291–299. [PubMed: 25264269]
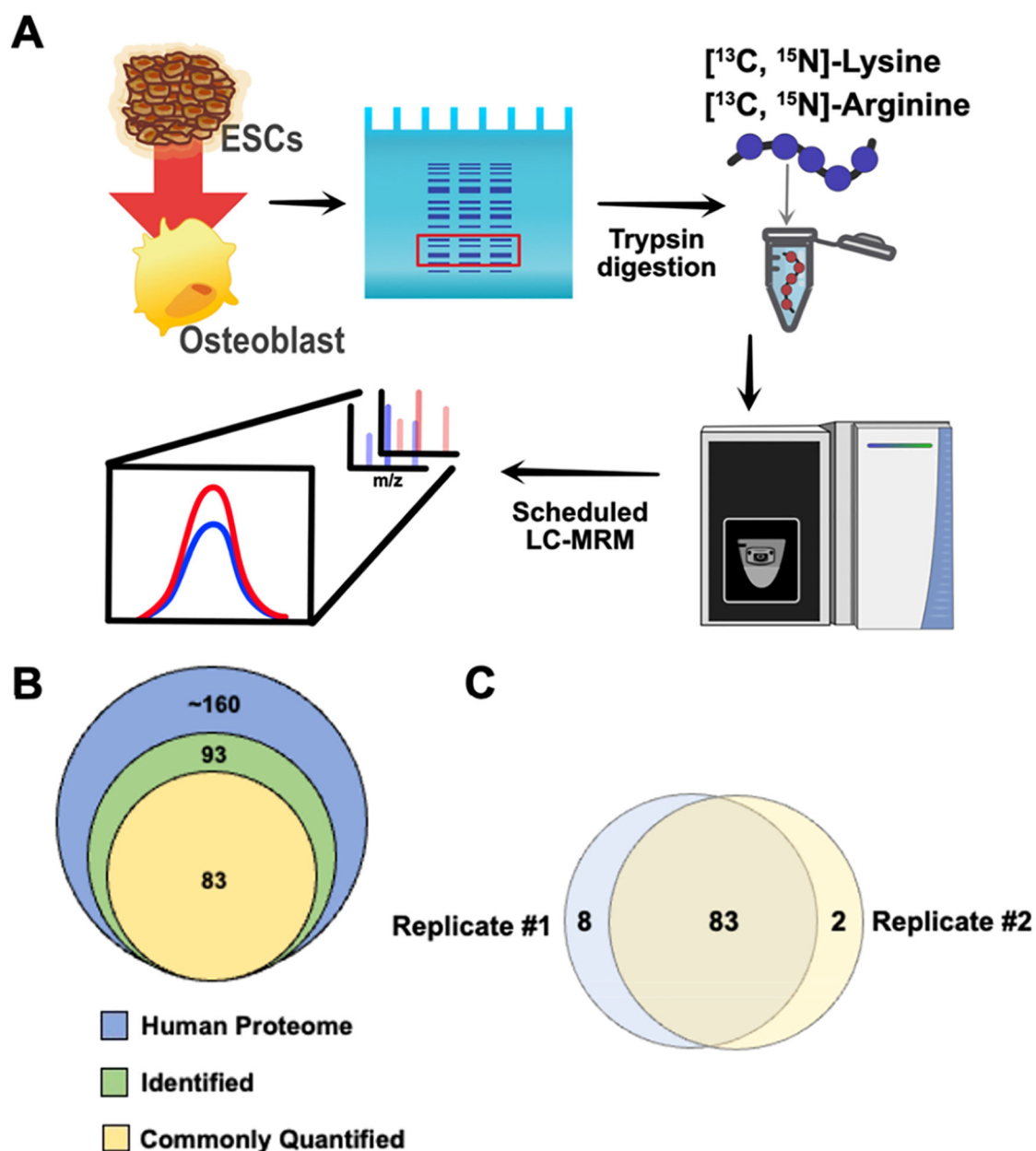
Figure 1.
High-throughput scheduled LC-MRM for quantifying small GTPase proteins during the osteogenic differentiation of H9 hESCs. (A) Schematic diagram illustrating the experimental workflow. Osteogenesis was induced in H9 hESCs, and the cells were collected at different time points. Total proteins were extracted for in-gel tryptic digestion, and the resulting peptides were spiked-in with a mixture of synthetic stable isotope-labeled small GTPase peptides of identical amino acid sequences prior to sample injection. The MRM data were analyzed using Skyline. (B) Venn diagram showing the numbers of small GTPases included in the MRM library, identified, and quantified by LC-MRM analysis. (C) Venn diagram displaying the number of commonly quantified small GTPase proteins in the two biological replicates.
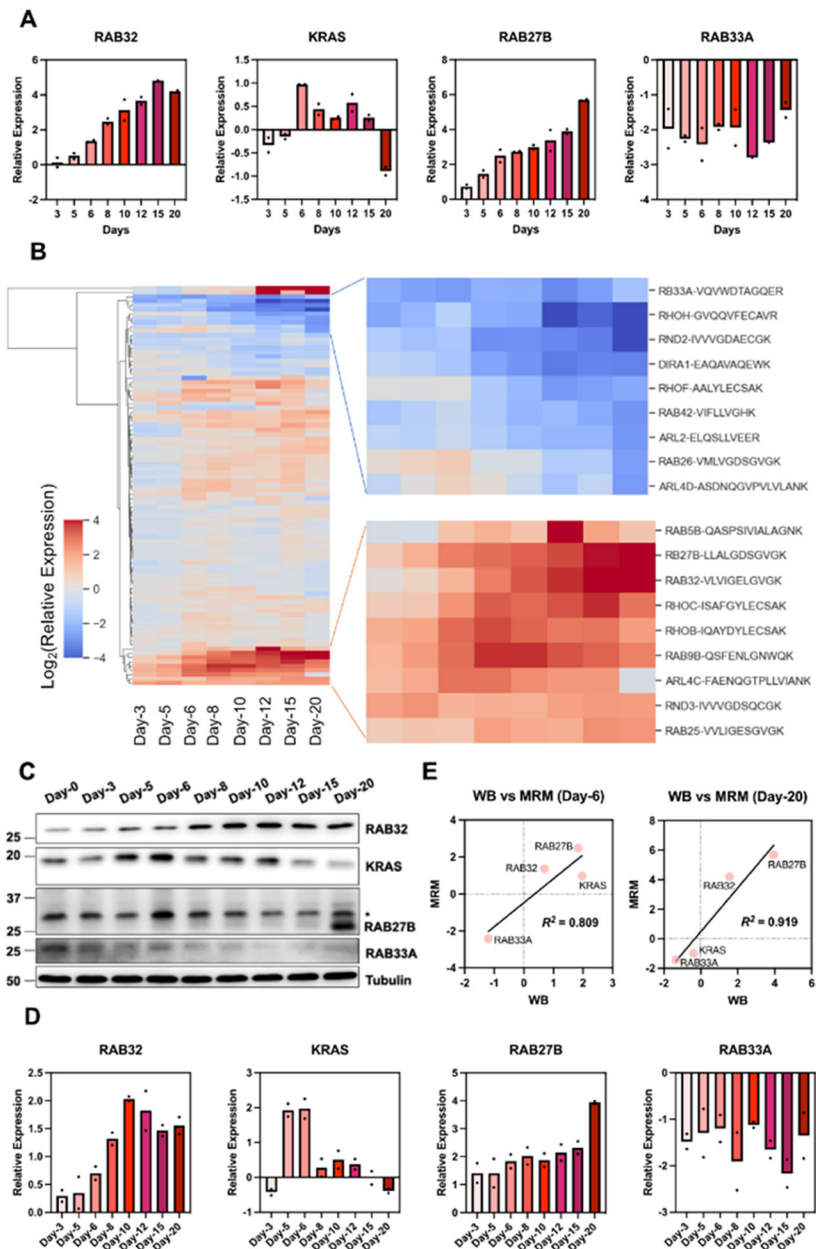
Figure 2.
Differential expression of small GTPases upon osteogenic differentiation of H9 hESCs.
(A) Bar charts showing profoundly altered expression of selected small GTPases,
including RAB32, KRAS, RAB27B, and RAB33A, during the time course of osteogenic
differentiation compared to day 0. The data represent average values, where the ratios
obtained from the two individual biological replicates are marked with dots. (B) Hierarchical
clustering heatmap in $\log_2$ ratio depicting the relative expression of small GTPase proteins
at different time points with respect to day 0. The corresponding unique peptides used for
quantification are listed after the protein name. (C) Western blot validations of the selected
small GTPases during the course of osteogenic differentiation of H9 hESCs. The nonspecific
band detected in the Western blot image of RAB27B is marked with an asterisk. (D) Bar

charts showing the quantification results of selected small GTPases. The signal intensities of the small GTPases were first normalized against that of tubulin, and the resulting ratios were further normalized against that of control (day 0). (E) Linear regression analysis of the relative expression of selected small GTPases measured by MRM and Western Blot analysis (WB) at day 6 or day 20.
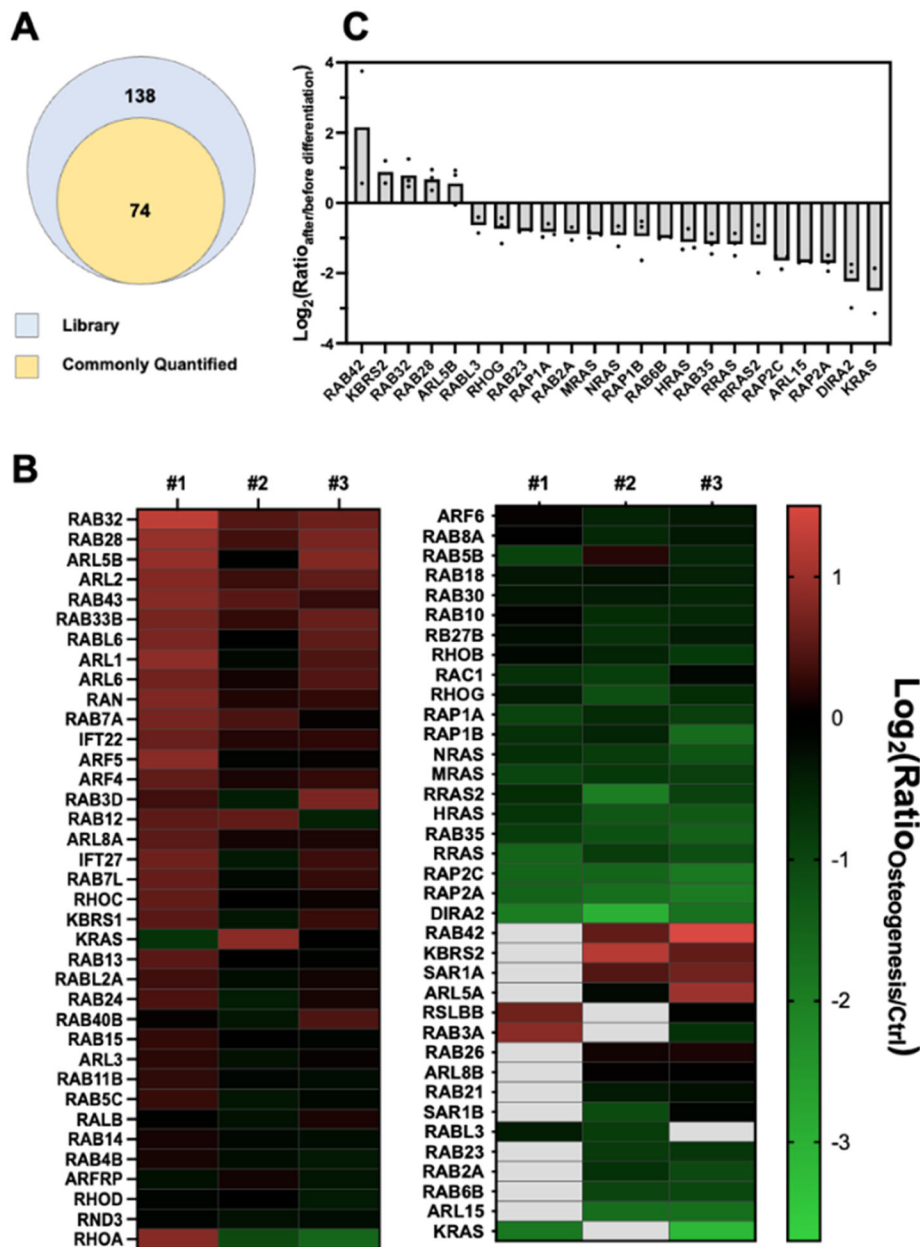
Figure 3.
Osteogenic differentiation of murine C3H10T1/2 mesenchymal progenitor cells. (A) Venn diagram showing the numbers of small GTPases commonly quantified in at least two biological replicates and in the library. (B) Heatmap showing the ratio of small GTPases during osteogenesis of C3H10T1/2 cells quantified from three biological replicates. Small GTPases with missing data are shown in gray boxes. (C) Bar chart displaying the differentially expressed small GTPases quantified in at least two biological replicates and with a cutoff ratio of 1.5-fold.
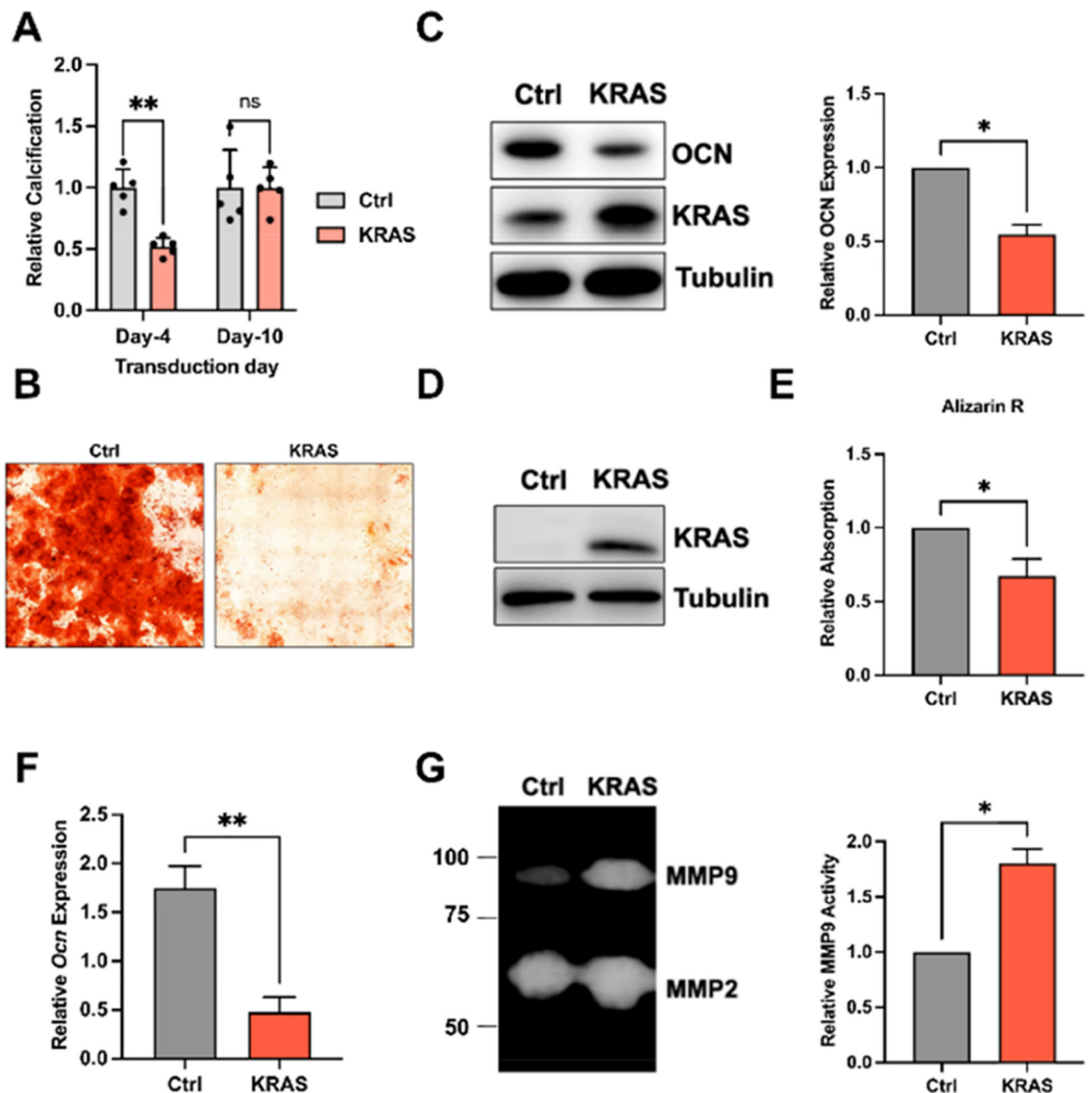
Figure 4.
KRAS regulates osteogenesis through modulating the integrity of extracellular matrix. (A) Bar chart displaying the results of calcium assay for H9 cells transduced with lentivirus at day 4 or day 10 for KRAS overexpression. (B) Alizarin Red S staining illustrating diminished osteogenesis rate of H9 cells overexpressing KRAS. (C) Western blot and the corresponding quantification results showing the successful overexpression of KRAS and the ensuing change in OCN expression in H9 cells at day 15 following transfection at day 4. (D) Western blot analysis showing the overexpression of KRAS in C3H10T1/2 cells. (E) Quantification results of Alizarin Red S staining showing the osteogenesis rate of C3H10T1/2 cells overexpressing KRAS. (F) RT-qPCR for the quantification of *Ocn* expression in C3H10T1/2 cells overexpressing KRAS. The level of *Ocn* mRNA was

normalized against that of *Gapdh* and further normalized against that of control (Ctrl). (G) Gel zymography analysis and the quantification results for the activity of secreted MMP9 from H9 cells overexpressing KRAS. The data represent mean ± S.D. of results obtained from three biological replicates. The *p*-values were calculated using two-tailed, unpaired *t*-test (*$0.05 < p < 0.01$; **$0.001 < p < 0.01$; ***$p < 0.001$; ns: $p > 0.05$).